

## Electron Heating by Lower Hybrid Waves in the PLT Tokamak

R. E. Bell, S. Bernabei, A. Cavallo, T. K. Chu, T. Luce, R. Motley, M. Ono, J. Stevens, and S. von Goeler

Princeton Plasma Physics Laboratory, Princeton, New Jersey 08544

(Received 8 June 1987)

Lower hybrid waves with a narrow, high-velocity wave spectrum have been used to achieve high central electron temperatures in a tokamak plasma. Waves with a frequency of 2.45 GHz launched by a sixteen-waveguide grill at a power level less than 600 kW were used to increase the central electron temperature of the PLT plasma from 2.2 to 5 keV. Associated with this temperature increase was an apparent reduction in the central electron thermal diffusivity. The magnitude of the temperature increase depends strongly on the phase difference between waveguides and on the direction of the launched wave.

PACS numbers: 52.50.Gj, 52.35.Hr, 52.55.Fa, 52.55.Pi

Lower hybrid (LH) waves have been applied to high-temperature tokamak plasmas demonstrating effects of current drive,<sup>1</sup> current start-up,<sup>2-4</sup> suppression of sawtooth oscillations,<sup>5-8</sup> and both electron and ion heating.<sup>9-13</sup> The experimental results presented here show that high central electron temperatures can be achieved with a modest power level under conditions that are also the most suitable for good current drive. Higher velocity waves with narrower wave spectra provide more efficient current drive,<sup>13</sup> and produce a larger increase in the central electron temperature, which decouples from the current profile.<sup>14</sup>

The experiment was carried out in the PLT tokamak which has a major radius  $R=132$  cm, a minor radius  $a=39$  cm, and a magnetic field  $B_T=3.1$  T. LH waves were launched with a sixteen-element grill with a narrow power spectrum ( $\Delta n_{\parallel}=0.45$  FWHM, where  $n_{\parallel}=ck_{\parallel}/\omega$ ). By adjustment of the relative phasing between adjacent waveguide elements, the peak value of  $n_{\parallel}$  was tuned between  $n_{\parallel 0}=1.4$  and 3.6, and the wave could be launched in the direction of the electron drift velocity (favoring current drive) or in the opposite direction (opposing the current). Ray-tracing calculations indicate that an upward shift in  $n_{\parallel}$  of  $\approx 10\%$  occurs on the first pass of the wave as it penetrates to the plasma center. The target plasmas had a line-averaged electron density  $\bar{n}_e=10^{13}$  cm<sup>-3</sup>, and the plasma current,  $I_p$ , was held constant (by adjustment of the current ramp rate in the Ohmic primary) during the application of 500–600 kW of LH power. The effective ionic charge of the plasma,  $Z_{\text{eff}}$ , was 3.4 (from Spitzer resistivity).

Electron temperature profiles for several phase differences, as measured along a vertical chord by a multipoint Thomson scattering system,<sup>15</sup> are compared in Fig. 1 to a profile before the application of rf power. (Each profile is the average of three consecutive plasma shots; for the Ohmic profile, six plasma shots with measurement times distributed throughout the phase of the sawtooth were used to give an average profile.) As the phase difference,  $\Delta\Phi$ , was varied from  $-180^\circ$  to  $-90^\circ$  (waves in the direction of the electron drift), the profile became more peaked, reaching a central electron tem-

perature,  $T_e(0)$ , of nearly 5 keV. [In other PLT experiments with similar conditions,  $T_e(0)$ 's above 6 keV were obtained.] Although there was a large change in the central temperature, the outer portion ( $r/a > 0.5$ ) of the profiles in all of these cases was similar. The inversion radius of sawteeth, as measured by electron cyclotron emission along the (horizontal) major radius, was  $r_{\text{inv}} \approx \pm 8$  cm about the plasma center for the Ohmic plasmas.

Figure 2 shows several plasma parameters during a shot with the waveguide grill phased for current drive ( $\Delta\Phi = -90^\circ$ ,  $n_{\parallel 0}=1.8$ ) with a launched power  $P_{\text{rf}}=585$  kW. The loop voltage,  $V_L$ , drops nearly to zero during the rf pulse. There was no increase in  $\bar{n}_e$  during the LH pulse, and the signal from the visible bremsstrahlung ( $I_{\text{brem}} \propto \langle n_e^2 Z_{\text{eff}} T_e^{-1/2} \rangle$ ) indicated no significant change in

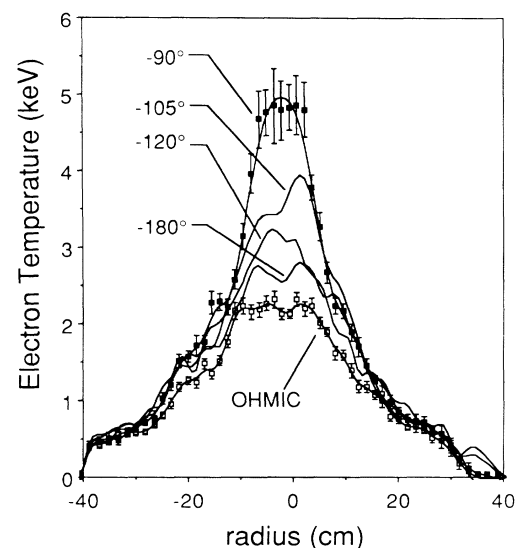


FIG. 1.  $T_e$  profiles measured at 600 ms by Thomson scattering comparing plasmas with no rf (open symbols) with the application of 500–600 kW of lower hybrid power at several waveguide phases. The phase differences  $-90^\circ$ ,  $-105^\circ$ ,  $-120^\circ$ , and  $-180^\circ$  correspond to  $n_{\parallel 0}$ 's of 1.8, 2.1, 2.4, and 3.6, respectively.

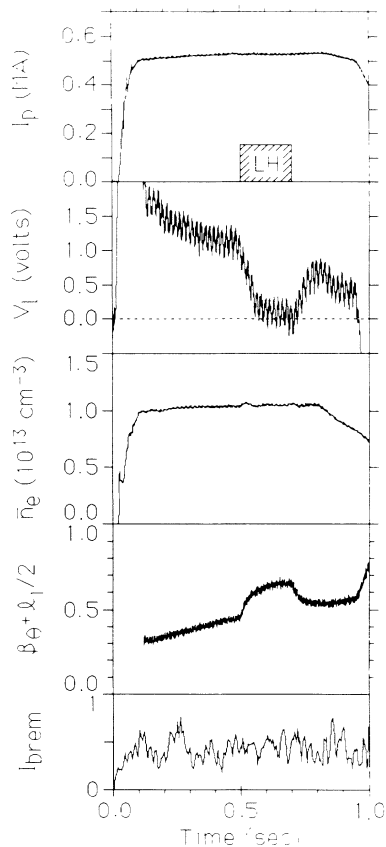


FIG. 2. Time history of some plasma parameters for waveguide phasing of  $\Delta\Phi = -90^\circ$ .

the effective charge ( $Z_{\text{eff}}$ ) of the plasma. (Since  $I_{\text{brem}}$  was a line-integrated signal, the  $T_e^{-1.2}$  dependence accounts for at most a 12% change in  $Z_{\text{eff}}$  for constant  $I_{\text{brem}}$ .) The rapid increase in the plasma equilibrium measurement of  $\Lambda = \beta_\theta + l_i/2$  at the beginning of the rf pulse was due primarily to an increase in  $\beta_\theta$ ,<sup>16</sup> due to a high-energy superthermal tail created by the LH waves. Any change in  $l_i$  occurred on a slower time scale during the rf pulse.

The increase in  $T_e(0)$  during the rf pulse over that of the Ohmic value can be seen in Fig. 3 as a function of  $\Delta\Phi$  [ $\Delta T_e(0) = T_e(0)_{\text{rf}} - T_e(0)_{\text{Ohmic}}$ ]. [Here  $T_e(0)$  is the average electron temperature  $\pm 3.5$  cm around the plasma center.] The solid data points have peak values of  $n_{\parallel}$  ranging between  $n_{\parallel 0} = 1.4$  ( $\Delta\Phi = -67.5^\circ$ ) and  $n_{\parallel 0} = 3.6$  ( $\Delta\Phi = -180^\circ$ ). A symmetric spectrum was produced by phasing adjacent waveguides  $00\pi\pi \dots 00\pi\pi$  such that the launched power was evenly divided between positive and negative lobes ( $n_{\parallel 0} = \pm 1.8$ ); the representation  $\Delta\Phi = \pm 90^\circ$  will be used for this spectrum (open points in Fig. 3). The rf power input was 500–600 kW, while the Ohmic power input was decreasing with decreasing  $n_{\parallel}$ . The symmetrically launched wave ( $\Delta\Phi = \pm 90^\circ$ ) results in a much lower  $T_e$  increase than one launched en-

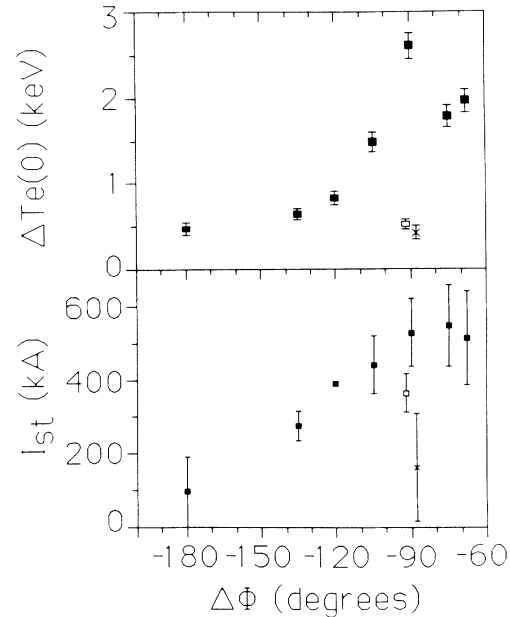


FIG. 3. Plot of  $\Delta T_e(0)$  and superthermal current vs waveguide phase difference. Solid symbols are for waves launched to drive current. Cross indicates waves launched to oppose current. Open symbols are for symmetrically launched waves.

tirely in the current-drive direction ( $\Delta\Phi = -90^\circ$ ). In another experiment, with a wave launched in the reverse (anticurrent) direction ( $\Delta\Phi = +90^\circ$ ) with similar power and plasma density, the temperature increase was also much lower (cross in Fig. 3) than that seen with waves launched in the current-drive direction.

The superthermal current generated by the waves was estimated, by a method similar to that of Chu *et al.*,<sup>17</sup> on the assumption that the  $Z_{\text{eff}}$  of the plasma did not change during the application of rf power. The voltage on axis,  $V_{\text{axis}}$ , was calculated from external circuits (Ohmic primary and vertical field) taking into account the change in  $LI_p^2/2$ . ( $\beta_\theta$  was not directly measured and was assumed to be constant during the rf after the initial rapid rise of  $\Lambda$ .) The resistivity,  $R_\Omega$ , of the thermal plasma was calculated from the  $T_e$  profile during the rf pulse with the value of  $Z_{\text{eff}}$  prior to the application of rf power. With the assumption of a uniform electric field, the estimated superthermal current (see Fig. 3) is then  $I_{\text{st}} = I_p - V/R_\Omega$ , where  $V$  is between  $V_L$  and  $V_{\text{axis}}$ . The error bars in Fig. 3 reflect the range of values of  $V$ .

The overall trend of increasing central temperature with lower  $n_{\parallel}$  correlates with the amount of superthermal current being driven. This is in contrast to what one would expect for the coupling between the superthermals and the bulk, i.e., the higher- $n_{\parallel}$  (lower energy) waves damp on lower-energy tail electrons which have a more efficient power transfer to the bulk. This might imply that the higher- $n_{\parallel}$  waves are damping at a larger radius and not penetrating to the plasma center, or that under

the conditions of strong current drive (and/or reduced electric field) there is an improvement in plasma conditions in the center as the superthermal current increases. The much higher  $\Delta T_e$  for  $\Delta\Phi = -90^\circ$  as compared with  $\Delta\Phi = \pm 90^\circ$ ,  $+90^\circ$  for which the damping should be similar also suggests that there is an improvement in central plasma confinement for waves launched to drive current. LH waves have been seen to suppress the sawteeth and to stabilize the  $m=1$  mode<sup>13</sup> and to reduce density fluctuations near the plasma center<sup>6</sup> during current drive, all of which may lead to reducing anomalous transport.

There is a peak in  $\Delta T_e$  at  $\Delta\Phi = -90^\circ$ . The faster wave spectra ( $\Delta\Phi = -75^\circ$  and  $-67.5^\circ$ ) have an increasing fraction of power inaccessible to the plasma center at this plasma density; the accessibility of the wave diminishes as  $n_{||}$  decreases. Approximately 5% of the  $\Delta\Phi = -75^\circ$  spectrum and 20% of the  $\Delta\Phi = -67.5^\circ$  spectrum were not accessible inside  $r=a/2$ . Also, faster wave spectra drive tail electrons to higher energy with slowing-down times approaching the tail confinement time resulting in decreased coupling to the bulk electrons (estimated to be a  $\approx 10\%$  effect). Together, these two effects may be responsible for the reduced  $\Delta T_e$  for  $\Delta\Phi > -90^\circ$ .

Sawteeth were present in these discharges before the LH power was applied. Sawteeth were suppressed in those discharges with  $-135^\circ \leq \Delta\Phi \leq -67.5^\circ$ , but were present in the reverse-current case ( $\Delta\Phi = +90^\circ$ ) and the symmetric cases ( $\Delta\Phi = \pm 90^\circ$ ,  $-180^\circ$ ). With only half the rf power of the  $\Delta\Phi = \pm 90^\circ$  case, LH waves with  $\Delta\Phi = -90^\circ$  ( $P_{rf} = 285$  kW) did suppress sawteeth. This asymmetry in the ability of the LH waves to suppress sawteeth has been observed previously.<sup>12</sup>

If the LH waves were heating by directly coupling to the bulk, better heating would be seen with slower waves (higher  $n_{||}$ ), provided that the slower waves penetrated into the plasma. Presumably, the LH wave deposits its power by damping on the superthermal tail electrons, which heat the bulk plasma by collisions with thermal electrons. The power deposition profile to the bulk electrons from the tail should be given approximately by the hard-x-ray profile, which was measured by an array of detectors along seven vertical chords ( $\hbar\nu > 35$  keV). Figure 4(a) compares the  $T_e^{3/2}$  profile of the Ohmic case with the Abel-inverted hard-x-ray profile on the current-driven plasma ( $\Delta\Phi = -90^\circ$ ). The power deposition profile could be narrower than that inferred from the hard-x-ray profile, since the x-ray emission is weighted by higher-energy electrons while power deposition is weighted towards lower energy.

A one-dimensional analysis was performed in order to examine the change in the electron thermal diffusivity,  $\chi_e$ , during LH current drive. The  $T_e$  and  $n_e$  profiles used were symmetrized and fitted with a smoothing cubic spline. It was assumed that all of the rf power was even-

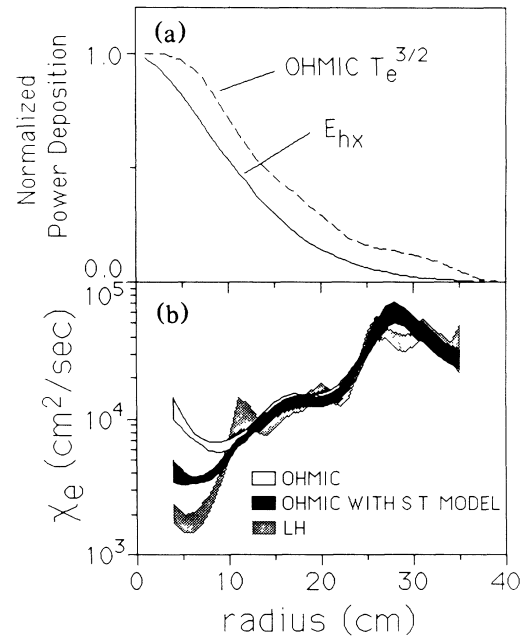


FIG. 4. (a)  $T_e^{3/2}$  profile for Ohmic discharge compared to Abel-inverted hard-x-ray profile during the lower hybrid pulse. (b) Calculated  $\chi_e(r)$  for the Ohmic plasma, Ohmic corrected for sawtooth transport, and during lower hybrid. The approximate position of the sawtooth inversion radius for the Ohmic plasma is 8 cm.

tually deposited in the bulk electrons, and the Abel-inverted-hard x-ray profile was used for the deposition profile. In this low-density discharge, energy losses by electrons to ions are negligible as are radiation losses from the central region of the plasma. In the Ohmic case, sawteeth were present, and so a simple model of the losses due to sawtooth transport was used to give an effective  $\chi_e$  averaged over a sawtooth period. The energy change inside  $r_{inv}$  ( $r \approx 8$  cm) during the rise of the sawtooth was estimated from the sawtooth amplitude measured by electron cyclotron emission ( $\approx 0.26$  keV in the Ohmic plasma). Dividing this energy by the sawtooth period ( $\approx 5.3$  ms) gave the average power needed to change the internal plasma kinetic energy. This power was equivalent to the average power expelled from the interior by sawteeth ( $\approx 40\%$  of the power deposited inside  $r_{inv}$ ).

Figure 4(b) compares the calculated  $\chi_e$  profiles for the Ohmic case (white), the Ohmic case corrected for sawtooth transport (black), and  $\Delta\Phi = -90^\circ$  LH case (shaded) shown in Fig. 1. The central value of  $\chi_e$  in the LH case ( $\chi_e^{LH}$ ) has decreased from the corrected Ohmic case ( $\chi_e^{Ohmic}$ ). The major source of uncertainty in  $\chi_e$  indicated in Fig. 4 is due primarily to the determination of  $dT/dr$  from the  $T_e$  profile. Also included are the uncertainties of the measured values of  $n_e$  and x-ray intensity and the uncertainty due to the inversion of the x-ray data. The use of the trapped-particle correction for the

Ohmic power deposition would give a more peaked power deposition than  $T_e^{3/2}$  thereby increasing  $\chi_e^{\text{Ohmic}}$ , and if the absorption efficiency of rf is less than unity or if there are direct losses from the superthermal tail,  $\chi_e^{\text{LH}}$  would decrease.

Alternatively, if one assumes that  $\chi_e^{\text{LH}} = \chi_e^{\text{Ohmic}}$ , then the power deposition for rf must be 30% narrower than that used above for  $\Delta\Phi = -90^\circ$  (low  $n_{\parallel}$ ); the power deposition must also broaden substantially as  $n_{\parallel}$  increases or changes sign to be consistent with the  $\Delta T_e$ 's of Fig. 3 (higher  $n_{\parallel}$ 's and  $\Delta\Phi = +90^\circ$  all have higher total input power and lower  $\Delta T_e$ 's). With no direct measurement of the power deposition to the bulk, the possibility of a power-deposition profile that is 30% narrower than that used to determine  $\chi_e$  cannot be ruled out; however, it is difficult to reconcile such a narrow power-deposition profile with the broader current profile expected with LH current drive.<sup>14</sup>

In conclusion, high central electron temperatures were achieved with a narrow  $n_{\parallel}$  spectrum of lower hybrid waves with low  $n_{\parallel}$  launched in the direction of the electron drift velocity. Waves launched to drive current produced much better electron heating than identical spectra launched symmetrically or in the anticurrent direction at a given  $n_{\parallel}$ , suggesting that the presence of a large superthermal current was necessary for electron heating. The elimination of sawteeth alone does not explain the large temperature rise since a large variation in central temperatures was observed even while no sawteeth existed, though the suppression of other activity (such as the  $m=1$  mode) with increasing superthermal current is a possible explanation. With use of the hard x rays to estimate a power deposition profile, a decrease in the central value of  $\chi_e$  from the Ohmic value was obtained for a lower hybrid plasma with a large superthermal current.

This work was supported by U.S. Department of Energy Contract No. DE-AC02-76-CHO-3073.

<sup>1</sup>N. J. Fisch, Phys. Rev. Lett. **41**, 873 (1978), and also Rev. Mod. Phys. **59**, 175 (1987), and references contained therein.

<sup>2</sup>F. Jobs *et al.*, Phys. Rev. Lett. **52**, 1005 (1984).

<sup>3</sup>K. Toi *et al.*, Phys. Rev. Lett. **52**, 2144 (1984).

<sup>4</sup>S. Kubo *et al.*, Phys. Rev. Lett. **50**, 1994 (1983).

<sup>5</sup>T. K. Chu *et al.*, in *Radiofrequency Plasma Heating—1985*, edited by D. G. Swanson, AIP Conference Proceedings No. 129 (American Institute of Physics, New York, 1985), p. 131.

<sup>6</sup>T. K. Chu *et al.*, Nucl. Fusion **26**, 666 (1986).

<sup>7</sup>C. Gormezano *et al.*, in Ref. 5, p. 111.

<sup>8</sup>K. McCormick *et al.*, in *Proceedings of the Twelfth European Conference on Controlled Fusion and Plasma Physics, Budapest, Hungary, 1985*, edited by L. Pocs and A. Montvai (European Physical Society, Petit-Lancy, Switzerland, 1985), Vol. 1, p. 199.

<sup>9</sup>F. Alladio *et al.*, in *Proceedings of the Ninth International Conference on Plasma Physics and Controlled Nuclear Fusion Research, Baltimore, Maryland, 1982* (IAEA, Vienna, Austria, 1983), Vol. 2, p. 41.

<sup>10</sup>M. Porkolab *et al.*, Phys. Rev. Lett. **53**, 1229 (1984).

<sup>11</sup>D. Van Houtte *et al.*, in *Proceedings of the Fourth International Symposium on Heating in Toroidal Plasmas, Rome, Italy, 1984*, edited by H. Knoepfel and E. Sindoni (International School of Plasma Physics, Varenna, Italy, 1984), Vol. 1, p. 554.

<sup>12</sup>F. Söldner *et al.*, in *Proceedings of the Thirteenth European Conference on Controlled Fusion and Plasma Physics, Schliersee, 1986*, edited by G. Briffod and M. Kaufmann (European Physical Society, Petit-Lancy, Switzerland, 1986), Vol. 2, p. 319.

<sup>13</sup>S. Bernabei *et al.*, in *Proceedings of the Eleventh International Conference on Plasma Physics and Controlled Nuclear Fusion Research, Kyoto, Japan, 1986* (IAEA, Vienna, 1987), Vol. 1, p. 503.

<sup>14</sup>K. McCormick *et al.*, Phys. Rev. Lett. **58**, 491 (1987).

<sup>15</sup>N. Bretz *et al.*, Appl. Opt. **17**, 192 (1978).

<sup>16</sup>S. Bernabei *et al.*, Bull. Am. Phys. Soc. **31**, 1466 (1986).

<sup>17</sup>T. K. Chu *et al.*, Nucl. Fusion **26**, 1319 (1986).

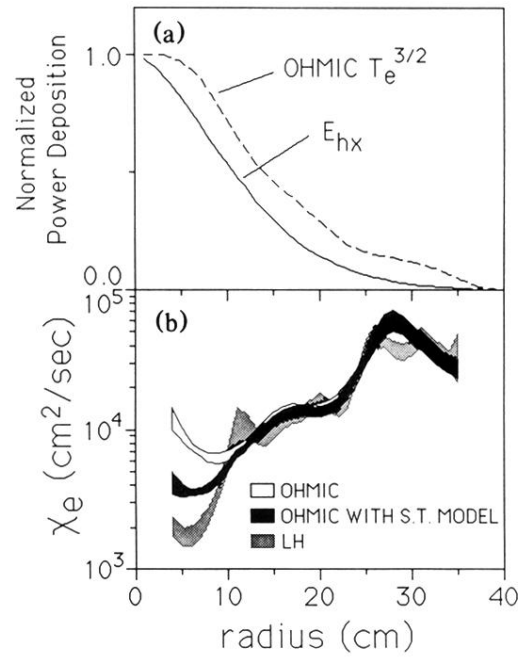


FIG. 4. (a)  $T_e^{3/2}$  profile for Ohmic discharge compared to Abel-inverted hard-x-ray profile during the lower hybrid pulse. (b) Calculated  $\chi_e(r)$  for the Ohmic plasma, Ohmic corrected for sawtooth transport, and during lower hybrid. The approximate position of the sawtooth inversion radius for the Ohmic plasma is 8 cm.